

# LIMIT POINTS AND HOPF BIFURCATION POINTS FOR A ONE - PARAMETER DYNAMICAL SYSTEM ASSOCIATED TO THE LUO - RUDY I MODEL

Cătălin Liviu Bichir\*    Adelina Georgescu<sup>†</sup>    Bogdan Amuzescu<sup>‡</sup>  
 Gheorghe Nistor<sup>§</sup>    Marin Popescu<sup>¶</sup>    Maria-Luiza Flonta<sup>||</sup>  
 Alexandru Dan Corlan\*\*    Istvan Svab<sup>††</sup>

## Abstract

A one - parameter dynamical system is associated to the mathematical problem governing the membrane excitability of a ventricular cardiomyocyte, according to the Luo-Rudy I model. An algorithm used to construct the equilibrium curve is presented. Some test functions are used in order to locate limit points and Hopf bifurcation points.

---

\*catalinliviubichir@yahoo.com, Rostirea Maths Research, Regimentul 11 Siret 27, Galați, Romania

<sup>†</sup>Academy of Romanian Scientists, Splaiul Independenței 54, Bucharest, Romania

<sup>‡</sup>bogdan@biologie.kappa.ro, Faculty of Biology, University of Bucharest, Splaiul Independenței 91-95, Bucharest, Romania. This research was partially supported from grant PNCDI2 61-010 to M-LF by the Romanian Ministry of Education, Research, and Innovation.

<sup>§</sup>University of Pitești, Str. Târgul din Vale 1, Pitești, Romania

<sup>¶</sup>University of Pitești, Str. Târgul din Vale 1, Pitești, Romania

<sup>||</sup>Faculty of Biology, University of Bucharest, Splaiul Independenței 91-95, Bucharest, Romania

\*\*Bucharest University Emergency Hospital, Splaiul Independenței 169, Bucharest, Romania

<sup>††</sup>Faculty of Biology, University of Bucharest, Splaiul Independenței 91-95, Bucharest, Romania

Two extended systems allow to calculate these points. The numerical results are presented in a bifurcation diagram.

**MSC:** 37N25 37G10 37M20.

**keywords:** limit point, Hopf bifurcation point, Luo-Rudy I model, arc-length-continuation method, Newton's method, computer program.

## 1 Introduction

The present paper is one of a series of research results, for the dynamical system associated to the Luo-Rudy I model, obtained under the coordination of Acad. Adelina Georgescu.

Mathematical models of cardiomyocyte electrophysiology based on experimentally determined kinetics of ion currents encompass over 40 years, since the early attempts of Denis Noble ([24], [25]) to accurate models of cell types in all regions of the heart that are now being incorporated into anatomically detailed models of the whole organ ([26]). These approaches introduced in successive steps several time-dependent ion current components, as well as a detailed dynamics of calcium in subcellular compartments, comprising release and reuptake from the sarcoplasmic reticulum ([5]), specific calcium buffers ([16]), and the electrogenic Na/Ca exchanger. The Luo-Rudy I model of ventricular cardiomyocyte ([22]), developed in the early 1990s starting from the Beeler-Reuter model ([1]), includes kinetics based on single-channel recordings. All current components are described by Hodgkin-Huxley type equations. This simplicity renders it adequate for mathematical analysis using methods of linear stability and bifurcation theory.

Nowadays, there exist numerous software packages for the numerical study of finite - dimensional dynamical systems, for example MATCONT, CL\_MATCONT, CL\_MATCONTM ([4], [13]), AUTO [6]. In this paper, numerical results are obtained by using some new computer programs.

## 2 Luo-Rudy I model

In spite of its simplicity, which comes from the fact that it does not take into account earlier findings concerning  $\text{Ca}^{2+}$  dynamics, the Luo-Rudy I model [22] proved to be very realistic, incorporating data derived from single-channel recordings obtained during the 1980s with the advent of the

patch-clamp technique ([15], [23]). The model comprises only three time and voltage-dependent ion currents (fast sodium current, slow inward current, time-dependent potassium current) plus three background currents (time-independent and plateau potassium current, background current). The Luo-Rudy I model reproduces a wealth of experimental findings, like: the fast upstroke velocity of the action potential ( $\dot{V}_{max} = 400$  V/sec), the behavior of the rising phase, late repolarization phase, and postrepolarization phase with changes in extracellular potassium concentration  $[K]_o$ , monotonic Wenckebach patterns and alternans at normal  $[K]_o$ , nonmonotonic Wenckebach periodicities, aperiodic patterns, and enhanced supernormal excitability resulting in unstable responses and chaotic activity at low  $[K]_o$ .

Let us briefly describe how different experimental facts were taken into account within the equations. The fast sodium current ( $I_{Na}$ ) incorporates both a slow process of recovery from inactivation and an adequate maximum conductance. The activation ( $m$ ) and inactivation ( $h$ ) rates are adapted from the Ebihara-Johnson  $I_{Na}$  model based on data from chicken embryo cardiac cells [7]. Two inactivation gates, fast and slow ( $h$  and  $j$ ) were used to render it compatible with single-channel data proving that near threshold potentials sodium channels tend to open several times during a depolarization (reopening phenomenon), and a significant fraction of channels do not open by the time of peak inward current. The start values of the slow inactivation gate  $j$  are obtained by setting  $j_\infty = h_\infty$ , as suggested by Haas *et al.* [14]. The slow inward current ( $I_{si}$ ) is represented exactly as in the Beeler-Reuter model. The time-dependent potassium current ( $I_K$ ) is controlled by a time-dependent activation gate ( $X$ ) and a time-independent inactivation gate ( $X_i$ ) with inward rectification properties, neither of which depends on  $[K]_o$ , while the single-channel conductance is proportional to the square root of  $[K]_o$ , as found in patch-clamp recordings on rabbit nodal cells [34]. The time-independent potassium current ( $I_{K1}$ ) is different from  $I_{K1}$  of the Beeler-Reuter model, featuring two important properties discovered by Sakmann and Trube using patch-clamp methods ([28], [29]): a square-root dependence of single-channel conductance on  $[K]_o$ , and a high selectivity for potassium, as well as the inactivation gate K1 identified by Kurachi in single-channel experiments [19]. Since this current inactivates completely during depolarization, the model was supplemented with two other time-independent potassium current components: a  $[K]_o$ -insensitive plateau current ( $I_{Kp}$ ), simulating the single-channel properties of the plateau current measured by Yue and Marban [36], and a background current ( $I_b$ ) with a reversal potential  $E_b = -59.87$  mV. We should remark that, although derived from single-channel experiments, the conductances, gating and re-

versal potentials of these three current components were adjusted using a parameter estimation technique to fit the whole-cell time-independent potassium current measured by Sakmann and Trube for different values of  $[K]_o$ . The mathematical problem governing the membrane excitability of a ventricular cardiomyocyte, according to the Luo-Rudy I model ([22]), is a Cauchy problem

$$u(0) = u_0, \quad (1)$$

for the system of first order ordinary differential equations

$$\frac{du}{dt} = \Phi(\eta, u), \quad (2)$$

where  $u = (u_1, \dots, u_8) = (V, [Ca]_i, h, j, m, d, f, X)$ ,  $\eta = (\eta_1, \dots, \eta_{13}) = (I_{st}, C_m, g_{Na}, g_{si}, g_{Kp}, g_b, [Na]_0, [Na]_i, [K]_0, [K]_i, PR_{NaK}, E_b, T)$ ,  $M = R^8$ ,  $\Phi : R^{13} \times M \rightarrow M$ ,  $\Phi = (\Phi_1, \dots, \Phi_8)$ ,

$$\begin{aligned} \Phi_1(\eta, u) = & -\frac{1}{\eta_2} [I_{st} + \eta_3 u_3 u_4 u_5^3 (u_1 - E_{Na}(\eta_7, \eta_8, \eta_{13})) \\ & + \eta_4 u_6 u_7 (u_1 - c_1 + c_2 \ln u_2) \\ & + g_K(\eta_{10}) X_i(u_1) (u_1 - E_K(\eta_7, \eta_8, \eta_9, \eta_{10}, \eta_{11}, \eta_{13})) u_8 \\ & + g_{K1}(\eta_{10}) K1_\infty(\eta_9, \eta_{10}, \eta_{13}, u_1) (u_1 - E_{K1}(\eta_9, \eta_{10}, \eta_{13})) \\ & + \eta_5 Kp(u_1) (u_1 - E_{Kp}(\eta_9, \eta_{10}, \eta_{13})) + \eta_6 (u_1 - \eta_{12})], \\ \Phi_2(\eta, u) = & -c_3 \eta_4 u_6 u_7 (u_1 - c_1 + c_2 \ln u_2) + c_4 (c_5 - u_2), \\ \Phi_\ell(\eta, u) = & \alpha_\ell(u_1) - (\alpha_\ell(u_1) + \beta_\ell(u_1)) u_\ell, \quad \ell = 3, \dots, 8. \end{aligned}$$

The definitions of variables  $V, [Ca]_i, h, j, m, d, f, X$ , parameters  $I_{st}, C_m, g_{Na}, g_{si}, g_{K1}, g_{Kp}, g_b, [Na]_0, [Na]_i, [K]_0, [K]_i, PR_{NaK}, E_b, T$ , constants  $c_1, \dots, c_5$ , functions  $g_K, E_{Na}, E_K, E_{K1}, E_{Kp}, K1_\infty, X_i, Kp, \alpha_\ell, \beta_\ell$ , default values of parameters and initial values of variables in the Luo-Rudy I model are:  $V$  - transmembrane potential,  $[Ca]_i$  - intracellular calcium concentration,  $h$  and  $j$  - fast and slow inactivation variable of  $I_{Na}$  (probability of gate  $h$  or  $j$  to be open),  $m$  - activation variable of  $I_{Na}$ ,  $d$  and  $f$  - activation and inactivation variable of  $I_{si}$ ,  $X$  - activation variable of  $I_K$ ,  $X_i$  - steady-state inactivation of  $I_K$ ,  $K1_\infty$  - steady-state gating variable of  $I_{K1}$ ,  $Kp$  - steady-state gating variable of  $I_{Kp}$ ,  $\alpha_\ell$  and  $\beta_\ell$  - voltage dependence of opening and closing rates expressed as Boltzmann distribution functions for two distinct energy levels,  $I_{st}$  - steady depolarizing/hyperpolarizing applied current,  $C_m$  - membrane capacitance per unit area,  $g_{Na}$  - maximal conductance of fast voltage-gated sodium current (per unit area),  $g_{si}$  - maximal conductance of slow inward (calcium) current,  $g_K$  - maximal conductance of time-dependent

potassium current,  $g_{K1}$  - maximal conductance of inward rectifier potassium current,  $g_{Kp}$  - maximal conductance of plateau potassium current,  $g_b$  - maximal conductance of background current,  $[Na]_0$ ,  $[Na]_i$ ,  $[K]_0$ ,  $[K]_i$  - extra- and intracellular concentrations of sodium and potassium,  $PR_{NaK}$  - sodium/potassium permeability ratio for  $I_K$ ,  $E_{Na}$ ,  $E_K$ ,  $E_{K1}$ ,  $E_{Kp}$ ,  $E_b$  - reversal potentials of  $I_{Na}$ ,  $I_K$ ,  $I_{K1}$ ,  $I_{Kp}$ ,  $I_b$ ,  $T$  - absolute temperature.

For the continuity of the model, the reader is referred to [21], and for the treatment of the vector field  $\Phi$  singularities to [3].  $\Phi$  is of class  $C^2$  on the domain of interest.

### 3 The one - parameter dynamical system associated to the Luo - Rudy I model

We performed the study of the dynamical system associated with the Cauchy problem (1), (2) by considering only the parameter  $\eta_1 = I_{st}$  and fixing the rest of parameters. Denote  $\lambda = \eta_1 = I_{st}$  and  $\eta_*$  the vector of the fixed values of  $\eta_2, \dots, \eta_{13}$ . Let  $F : R \times M \rightarrow M$ ,  $F(\lambda, u) = \Phi(\lambda, \eta_*, u)$ ,  $F = (F_1, \dots, F_8)$ . Consider the dynamical system associated with the Cauchy problem (1), (3), where

$$\frac{du}{dt} = F(\lambda, u). \quad (3)$$

The equilibrium points of this problem are solutions of the equation

$$F(\lambda, u) = 0. \quad (4)$$

The existence of the solutions and the number were established by graphical representation in [3], for the domain of interest. The equilibrium curve (the bifurcation diagram) was obtained in [3], via an arc-length-continuation method ([11]) and Newton's method ([10]), starting from a solution obtained by solving a nonlinear least-squares problem ([11]) for a value of  $\lambda$  for which the system has one solution. In [3], the results are obtained by reducing (4) to a system of two equations in  $(u_1, u_2) = (V, [Ca]_i)$ . Here, we used directly (4).

### 4 Arc-length-continuation method and Newton's method for (4)

Let us write the arc-length-continuation method and Newton's method used to construct the equilibrium curve of (4).

Glowinski ([11], following H.B.Keller [17], [18]) chose a continuation equation written in our case as

$$\sum_{i=1}^8 \left( \frac{du_i}{ds} \right)^2 + \left( \frac{d\lambda}{ds} \right)^2 = 1, \quad (5)$$

where  $s$  is the curvilinear abscissa.

Let  $(\lambda_*, u_*)$  be a solution of (4) obtained by solving a nonlinear least-squares problem ([11]) for a fixed value of  $\lambda$  ( $\lambda = \lambda_*$ ) for which the system has one solution. To solve (4), let us consider the extended system formed by (4) and (5), parameterized by  $s$ . Let  $\Delta s$  be an arc-length step and  $u^n \cong u(n\Delta s)$ . We have the algorithm (following the case formulated in [11]): take  $\lambda(0) = \lambda^0 = \lambda_*$ ,  $u(0) = u^0 = u_*$  and suppose that  $\frac{d\lambda(0)}{ds}$ ,  $\frac{du(0)}{ds}$  are given; for  $n \geq 0$ , assuming that  $\lambda^{n-1}$ ,  $u^{n-1}$ ,  $\lambda^n$ ,  $u^n$  are known,  $(\lambda^{n+1}, u^{n+1})$  is obtained by

$$F(\lambda^{n+1}, u^{n+1}) = 0 \quad (6)$$

and

$$\begin{aligned} \sum_{i=1}^8 (u_i^1 - u_i^0) \frac{du_i(0)}{ds} + (\lambda^1 - \lambda^0) \frac{d\lambda(0)}{ds} &= \Delta s \text{ if } n = 0, \\ \sum_{i=1}^8 (u_i^{n+1} - u_i^n) \frac{u_i^n - u_i^{n-1}}{\Delta s} + (\lambda^{n+1} - \lambda^n) \frac{\lambda^n - \lambda^{n-1}}{\Delta s} &= \Delta s \text{ if } n \geq 1. \end{aligned} \quad (7)$$

In order to calculate  $\frac{d\lambda(0)}{ds}$ ,  $\frac{du(0)}{ds}$ , we obtain the following relations. From (4), we have

$$\sum_{i=1}^8 \frac{\partial F_j(\lambda^0, u^0)}{\partial u_i} \frac{du_i(0)}{ds} + \frac{\partial F_j(\lambda^0, u^0)}{\partial \lambda} \frac{d\lambda(0)}{ds} = 0, \quad j = 1, \dots, 8. \quad (8)$$

Let

$$\frac{du_i(0)}{ds} = \hat{u}_i \frac{d\lambda(0)}{ds}, \quad i = 1, \dots, 8. \quad (9)$$

$\hat{u} = (\hat{u}_1, \dots, \hat{u}_8)$  is the solution of

$$\sum_{i=1}^8 \frac{\partial F_j(\lambda^0, u^0)}{\partial u_i} \hat{u}_i = - \frac{\partial F_j(\lambda^0, u^0)}{\partial \lambda}, \quad j = 1, \dots, 8. \quad (10)$$

From (5), we have

$$\left(\sum_{i=1}^8 \hat{u}_i + 1\right) \left(\frac{d\lambda(0)}{ds}\right)^2 = 1. \quad (11)$$

In (7), let us denote  $u^* = u^0$ ,  $\lambda^* = \lambda^0$ ,  $u^{**} = \frac{du(0)}{ds}$ ,  $\lambda^{**} = \frac{d\lambda(0)}{ds}$  if  $n = 0$  and  $u^* = u^n$ ,  $\lambda^* = \lambda^n$ ,  $u^{**} = \frac{u^n - u^{n-1}}{\Delta s}$ ,  $\lambda^{**} = \frac{\lambda^n - \lambda^{n-1}}{\Delta s}$  if  $n \geq 1$ .

The algorithm which we use to construct the branch of solutions for (4) is the following:

1. given  $\lambda^0, u^0$ , solve (10) to obtain  $\hat{u}$ ;
2. obtain  $\frac{d\lambda(0)}{ds}$  from (11) and  $\frac{du(0)}{ds}$  from (9);
3.  $\lambda(0) = \lambda^0 = \lambda_*$  and  $u(0) = u^0 = u_*$  are taken as discussed above; for  $n \geq 0$ , taking  $\lambda^n, u^n$  as initial iteration, the following algorithm based on Newton's method calculates  $\lambda^{n+1}, u^{n+1}$ : obtain  $(\lambda^{m+1}, u^{m+1})$  using

$$\begin{aligned} & \sum_{i=1}^8 \frac{\partial F_j(\lambda^m, u^m)}{\partial u_i} u_i^{m+1} + \frac{\partial F_j(\lambda^m, u^m)}{\partial \lambda} \lambda^{m+1} \\ &= \sum_{i=1}^8 \frac{\partial F_j(\lambda^m, u^m)}{\partial u_i} u_i^m + \frac{\partial F_j(\lambda^m, u^m)}{\partial \lambda} \lambda^m \\ & \quad - F_j(\lambda^m, u^m), \quad j = 1, \dots, 8 \\ & \sum_{i=1}^8 u_i^{**} u_i^{m+1} + \lambda^{**} \lambda^{m+1} = \sum_{i=1}^8 u_i^* u_i^{**} + \lambda^* \lambda^{**} + \Delta s; \end{aligned} \quad (12)$$

calculate the eigenvalues of the Jacobian matrix  $D_u F(\lambda^{n+1}, u^{n+1})$  by the QR algorithm, calculate  $\psi_{LP}(\lambda^{n+1}, u^{n+1})$  by (13), and calculate  $\psi_H(\lambda^{n+1}, u^{n+1})$  by (14);

4. the algorithm is stopped after an imposed number of iterations for  $n$ .

## 5 Limit points and Hopf bifurcation points

In order to locate the limit points and the Hopf bifurcation points on the equilibrium curve of (4), two test functions ([20], [12], [32], [33]),  $\psi_{LP}$  and  $\psi_H$ , are evaluated at each iteration  $(\lambda^{n+1}, u^{n+1})$  of the algorithm from the end of section 4, where

$$\psi_{LP}(\lambda, u) = \det(D_u F(\lambda, u)), \quad (13)$$

$$\psi_H(\lambda, u) = \det(2 D_u F(\lambda, u) \odot I_8). \quad (14)$$

$\psi_H$  is evaluated using formula (15). For a  $n \times n$  matrix  $A$  with elements  $\{a_{ij}\}$ , the following  $m \times m$  matrix,  $m = \frac{1}{2}n(n-1)$ , is obtained ([20], [12]) based on the definition of the bialternate product  $\odot$  of two matrices,

$$(2A \odot I_n)_{(p,q),(r,s)} = \begin{cases} -a_{ps}, & \text{if } r = q, \\ a_{pr}, & \text{if } r \neq p \text{ and } s = q, \\ a_{pp} + a_{qq}, & \text{if } r = p \text{ and } s = q, \\ a_{qs}, & \text{if } r = p \text{ and } s \neq q, \\ -a_{qr}, & \text{if } s = p, \\ 0, & \text{otherwise.} \end{cases} \quad (15)$$

The rows are labeled by the multi-index  $(p, q)$  ( $p = 2, 3, \dots, n, q = 1, 2, \dots, p-1$ ), and the columns are labeled by the multi-index  $(r, s)$  ( $r = 2, 3, \dots, n, s = 1, 2, \dots, r-1$ ).

If  $\psi_{LP}$  has opposite signs at two points  $(\lambda^n, u^n)$  and  $(\lambda^{n+1}, u^{n+1})$ , then a limit point exists between  $(\lambda^n, u^n)$  and  $(\lambda^{n+1}, u^{n+1})$ . If  $\psi_H$  has opposite signs at these two points, then it is possible that a Hopf bifurcation point exists between them. The existence of a Hopf bifurcation point is decided by studying the form of eigenvalues of  $D_u F(\lambda^n, u^n)$  and of  $D_u F(\lambda^{n+1}, u^{n+1})$ , since  $\psi_H$  can be zero if there is a pair of real eigenvalues of opposite sign and with equal modulus. (We had in view the existence of a pair of complex conjugate eigenvalues, for each matrix, and a change of the sign of their real part).

For the cases where the test functions detect a limit point or a Hopf bifurcation point, we retain the results of one of the iterations  $(\lambda^n, u^n)$  or  $(\lambda^{n+1}, u^{n+1})$  of the algorithm presented at the end of section 4, namely the iteration where the modulus of the test function is smaller. These results are an initial iteration for Newton's method applied to one of the equations ([31], [32], [33])

$$G(\lambda, u, h) = 0, \quad (16)$$

$$H(\lambda, \beta, u, h, g) = 0. \quad (17)$$

The components  $(\lambda, u)$  of the solution of (16) represent a limit point of (4). The components  $(\lambda, u)$  of the solution of (17) represent a Hopf bifurcation point of (3).  $H$  and  $G$  are defined by

$$G : R^{2 \cdot 8 + 1} \rightarrow R^{2 \cdot 8 + 1}, \quad G(\lambda, u, h) = \begin{bmatrix} F(\lambda, u) \\ D_u F(\lambda, u)h \\ h_k - 1 \end{bmatrix}, \quad (18)$$



$$H : R^{3 \cdot 8 + 2} \rightarrow R^{3 \cdot 8 + 2}, H(\lambda, \beta, u, h, g) = \begin{bmatrix} F(\lambda, u) \\ D_u F(\lambda, u)h + \beta g \\ D_u F(\lambda, u)g - \beta h \\ h_k - 1 \\ g_k \end{bmatrix}, \quad (19)$$

where  $k$  is a fixed index,  $1 \leq k \leq 8$ . The extended system (17) determines a Hopf bifurcation point  $(\lambda, u)$ , a pair of purely imaginary eigenvalues  $\pm \beta i$  of the Jacobian matrix in  $(\lambda, u)$ , and a nonzero complex vector  $h + ig$ . Newton's method applied to the equation (16) is: let  $v^0 = (\lambda^0, u^0, h^0)$  be an initial iteration, where  $\lambda^0, u^0$  are as specified above and  $h^0 = (1, 0, 0, 0, 0, 0, 0, 0)$ ;  $k = 1$ ; for  $m \geq 0$ , calculate  $v^{m+1} = (\lambda^{m+1}, u^{m+1}, h^{m+1})$  using

$$DG(v^m)(v^{m+1} - v^m) = -G(v^m). \quad (20)$$

Newton's method applied to the equation (17) leads to: let  $w^0 = (\lambda^0, \beta^0, u^0, h^0, g^0)$  be an initial iteration, where  $\lambda^0, u^0$  are as specified above,  $\beta^0$  is the positive complex part of one of the two complex conjugate eigenvalues of the Jacobian matrix in  $(\lambda^0, u^0)$ ,  $h^0 = (1, 0, 0, 0, 0, 0, 0, 0)$ ,  $g^0 = (0, 0, 0, 0, 0, 0, 0, 0)$ ;  $k = 1$ ; for  $m \geq 0$ , calculate  $w^{m+1} = (\lambda^{m+1}, \beta^{m+1}, u^{m+1}, h^{m+1}, g^{m+1})$  using

$$DH(w^m)(w^{m+1} - w^m) = -H(w^m). \quad (21)$$

## 6 Numerical results

Based on the computer program for [2], the algorithm at the end of section 4 was transformed into a new computer program. Two new computer programs were written in order to solve (16) and (17) by (20) and (21) respectively.

We took  $C_m = 1$ ,  $g_{Na} = 23$ ,  $g_{si} = 0.09$ ,  $g_K = 0.282$ ,  $g_{K1} = 0.6047$ ,  $g_{Kp} = 0.0183$ ,  $G_b = 0.03921$ ,  $[Na]_0 = 140$ ,  $[Na]_i = 18$ ,  $[K]_0 = 5.4$ ,  $[K]_i = 145$ ,  $PR_{NaK} = 0.01833$ ,  $E_b = -59.87$ ,  $T = 310$ .

The equilibrium curves (the bifurcation diagram) are presented in figure 1 for the domain of interest. The variation of the functions  $\psi_{LP}$  and  $\psi_H$  are also represented. "LP1" and "LP2" indicate two limit points. "H" indicates a Hopf bifurcation point.

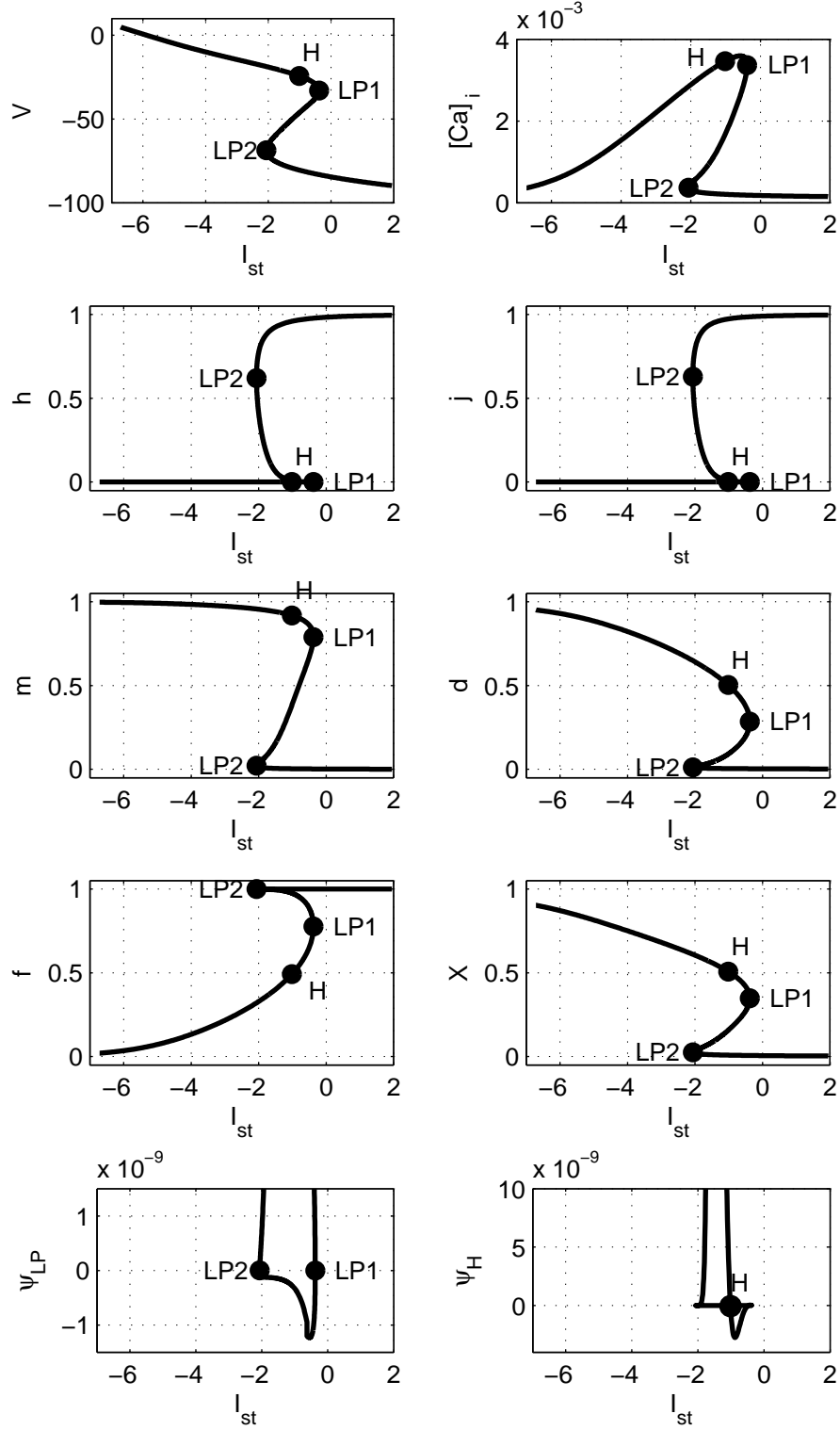


Figure 1: The bifurcation diagram and the variation of  $\psi_{LP}$  and  $\psi_H$ . There exist two limit points (LP1, LP2) and a Hopf bifurcation point (H).

The behavior of the dynamical system changes with the value of the variable parameter  $I_{st}$ . The two limit points separate three branches of stationary solutions (first graph in Fig. 1). While solutions on the middle branch (according to values of  $V$ ) are always unstable and those on the lower branch are always stable, on the upper branch there is a region where the system features oscillatory behavior. Oscillations are either damped, at the left of the Hopf bifurcation point, or amplified until the system falls on the lower branch of solutions to the right of the Hopf bifurcation. Amplified oscillations represent early afterdepolarizations (EADs), a condition prone to result in life-threatening arrhythmias. A recent study of the Luo-Rudy I dynamical system for variable relaxation time constants of the gating variables  $d$ ,  $f$ , and  $X$  ([35]), has proved that oscillations resulting in EADs appear above a Hopf bifurcation point for a fast subsystem, comprising the variables  $V$ ,  $d$ , and  $f$ . Moreover, these EADs can result in chaotic behavior when the system is paced at a constant cycle length. The same group has shown on detailed three-dimensional ventricular electrophysiology models that EADs occurring in certain regions can synchronize, resulting in polymorphic ventricular tachycardia or torsades-de-pointes ([30]).

In conclusion, our study, focused on analysis of the Luo-Rudy I system as a whole in conditions of variable parameter  $I_{st}$ , has identified two limit points and a Hopf bifurcation point, separating different regions of stability, some of them featuring amplified self-sustained oscillations defined as EADs on the time trajectories, and which may result in dangerous ventricular arrhythmias by synchronization. In contrast to the majority of previous arrhythmogenesis studies, which attributed the generation of this phenomenon to an individual condition, such as altered gating of an ion channel type due to gene mutations or modulation by physiological or pharmacological mechanisms, our results prove that arrhythmogenesis may result as an emergent feature of the system as a whole, and not of its individual components.

## References

- [1] G. W. Beeler , H. Reuter, Reconstruction of the action potential of ventricular myocardial fibres. *J. Physiol.* **268**:177-210, 1977.
- [2] C. L. Bichir, A numerical study by FEM and FVM of a problem which presents a simple limit point. *ROMAI J.* **4**(2):45-56, 2008. <http://www.romai.ro>, <http://rj.romai.ro>.

- [3] C. L. Bichir, B. Amuzescu, A. Georgescu, M. Popescu, Ghe. Nistor, I. Svab, M. L. Flonta, A. D. Corlan, Stability and self-sustained oscillations in a ventricular cardiomyocyte model. Submitted to *Interdisciplinary Sciences: Computational Life Sciences*, Springer.
- [4] A. Dhooge, W. Govaerts, Yu.A. Kuznetsov, W. Mestrom, A.M. Riet, B. Sautois, *MATCONT and CL-MATCONT: Continuation toolboxes in MATLAB*. 2006, <http://www.matcont.ugent.be/manual.pdf>
- [5] D. DiFrancesco , D. Noble, A model of cardiac electrical activity incorporating ionic pumps and concentration changes. *Philos. Trans. R. Soc. Lond. B Biol. Sci.* **307**:353-398, 1985.
- [6] E. Doedel, *Lecture Notes on Numerical Analysis of Nonlinear Equations*. 2007, <http://cmvl.cs.concordia.ca/publications/notes.ps.gz>, from the Home Page of the AUTO Web Site, <http://indy.cs.concordia.ca/auto/>.
- [7] L. Ebihara, E. A. Johnson, Fast sodium current in cardiac muscle. A quantitative description.(in French) *Biophys. J.* **32**:779-790, 1980.
- [8] A.Georgescu, M.Moroianu, I.Oprea, *Bifurcation Theory. Principles and Applications*. Applied and Industrial Mathematics Series, **1**, University of Pitesti, 1999.
- [9] W. J. Gibb , M. B. Wagner, M. D. Lesh, Effects of simulated potassium blockade on the dynamics of triggered cardiac activity. *J. Theor. Biol.* **168**:245-257, 1994.
- [10] V.Girault, P.-A.Raviart, *Finite Element Methods for Navier-Stokes Equations.Theory and Algorithms*. Springer, Berlin, 1986.
- [11] R.Glowinski, *Numerical Methods for Nonlinear Variational Problems*. Springer, New York, 1984.
- [12] W.J.F. Govaerts, *Numerical Methods for Bifurcations of Dynamical Equilibria*. SIAM, Philadelphia, 2000.
- [13] W. Govaerts, Yu. A. Kuznetsov R. Khoshsiar Ghaziani, H.G.E. Meijer, *CL\_MatContM: A toolbox for continuation and bifurcation of cycles of maps*. 2008, [http://www.matcont.ugent.be/doc\\_cl\\_matcontM.pdf](http://www.matcont.ugent.be/doc_cl_matcontM.pdf)
- [14] H. G. Haas, R. Kern, H. M. Einwachter and M. Tarr, Kinetics of Na inactivation in frog atria. *Pflügers Arch.* **323**:141-157, 1971.

- [15] O. P. Hamill, A. Marty, E. Neher, B. Sakmann and F. J. Sigworth, Improved patch-clamp techniques for high-resolution current recording from cells and cell-free membrane patches. *Pflügers Arch.* **391**:85-100, 1981.
- [16] D. W. Hilgemann, D. Noble, Excitation-contraction coupling and extracellular calcium transients in rabbit atrium: reconstruction of basic cellular mechanisms. *Proc. R. Soc. Lond. B Biol. Sci.* **230**:163-205, 1987.
- [17] H.B.Keller, *Numerical Solution of Bifurcation Eigenvalue Problems*. in *Applications in Bifurcation Theory*. ed. by P.Rabinowitz, Academic, New York, 1977.
- [18] H.B.Keller, *Global Homotopies and Newton Methods*. in *Recent Advances in Numerical Methods*. ed. by C. de Boor, G.H. Golub, Academic Press, New York, 1978.
- [19] Y. Kurachi, Voltage-dependent activation of the inward-rectifier potassium channel in the ventricular cell membrane of guinea-pig heart. *J. Physiol.* **366**:365-385, 1985.
- [20] Yu. A. Kuznetsov, *Elements of Applied Bifurcation Theory*. Springer, New York, 1998.
- [21] L. Livshitz, Y. Rudy, Uniqueness and stability of action potential models during rest, pacing, and conduction using problem - solving environment. *Biophysical J.* **97**:1265-1276, 2009.
- [22] C.H. Luo, Y. Rudy, A model of the ventricular cardiac action potential. Depolarization, repolarization, and their interaction. *Circ. Res.* **68**:1501-1526, 1991.
- [23] E. Neher, B. Sakmann, Single-channel currents recorded from membrane of denervated frog muscle fibres. *Nature* **260**:799-802, 1976.
- [24] D. Noble, Cardiac action and pacemaker potentials based on the Hodgkin-Huxley equations. *Nature* **188**:495-497, 1960.
- [25] D. Noble, A modification of the Hodgkin-Huxley equations applicable to Purkinje fibre action and pace-maker potentials. *J. Physiol.* **160**:317-352, 1962.

- [26] D. Noble, Modelling the heart: insights, failures and progress. *Bioessays* **24**:1155-1163, 2002.
- [27] T.S.Parker, L.O.Chua, *Practical Numerical Algorithms for Chaotic Systems*. Springer, New York, 1989.
- [28] B. Sakmann, G. Trube, Conductance properties of single inwardly rectifying potassium channels in ventricular cells from guinea-pig heart. *J. Physiol.* **347**:641-657, 1984.
- [29] B. Sakmann, G. Trube, Voltage-dependent inactivation of inward-rectifying single-channel currents in the guinea-pig heart cell membrane. *J. Physiol.* **347**:659-683, 1984.
- [30] D. Sato, L.-H. Xie, A. A. Sovari, D. X. Tran, N. Morita, F. Xie, H. Karagueuzian, A. Garfinkel, J. N. Weiss, Z. Qu, Synchronization of chaotic early afterdepolarizations in the genesis of cardiac arrhythmias. *PNAS* **106**:2983-2988, 2009.
- [31] R. Seydel, Numerical computation of branch points in nonlinear equations. *Numer. Math.* **33**:339-352, 1979.
- [32] R. Seydel, *Nonlinear Computation*. invited lecture and paper presented at the Distinguished Plenary Lecture session on Nonlinear Science in the 21st Century, 4th IEEE International Workshops on Cellular Neural Networks and Applications, and Nonlinear Dynamics of Electronic Systems, Sevilla, June, 26, 1996.
- [33] R. Seydel, *Practical Bifurcation and Stability Analysis*. Springer, New York, 2010.
- [34] T. Shibasaki, Conductance and kinetics of delayed rectifier potassium channels in nodal cells of the rabbit heart. *J. Physiol.* **387**:227-250, 1987.
- [35] D. X. Tran, D. Sato, A. Yochelis, J. N. Weiss, A. Garfinkel, Z. Qu, Bifurcation and chaos in a model of cardiac early afterdepolarizations. *Phys. Rev. Lett.* **102**:258103(4), 2009.
- [36] D. T. Yue, E. Marban, A novel cardiac potassium channel that is active and conductive at depolarized potentials. *Pflügers Arch.* **413**:127-133, 1988.